# Turbulence in the swash and surf zones: a review

Sandro Longo [a,*], Marco Petti [b,1], Inigo J. Losada [c,2]

[a]*Department of Civil Engineering, University of Parma, Parco Area delle Scienze, 181/A, 43100 Parma, Italy*
[b]*Dipartimento di Georisorse e Territorio, Faculty of Engineering, University of Udine, Via del Cotonificio, 114, 33100 Udine, Italy*
[c]*Ocean and Coastal Research Group, Universidad de Cantabria, E.T.S.I.C.C. y P. Av. de los Castros s/n, 39005 Santander, Spain*

## Abstract

This paper reviews mainly conceptual models and experimental work, in the field and in the laboratory, dedicated during the last decades to studying turbulence of breaking waves and bores moving in very shallow water and in the swash zone. The phenomena associated with vorticity and turbulence structures measured are summarised, including the measurement techniques and the laboratory generation of breaking waves or of flow fields sharing several characteristics with breaking waves. The effect of air entrapment during breaking is discussed. The limits of the present knowledge, especially in modelling a two- or three-phase system, with air and sediment entrapped at high turbulence level, and perspectives of future research are discussed. © 2002 Elsevier Science B.V. All rights reserved.

*Keywords:* Swash zone; Surf zone; Breaking waves; Turbulence; Length scales; Coastal hydrodynamics

## 1. Introduction

The swash zone is defined as the part of the beach between the minimum and maximum water levels during wave runup and rundown. Often the single term runup includes both uprush and backwash and is intended to mean the movement of the waterline on the beach.

Several authors prefer to consider the swash as the fluctuating component of the shoreline motion superimposed on a quasi-steady superelevation of the water level called setup. Sometimes it is considered the extreme region of the inner surf zone, where a large range of scales and types of fluid motions, including short and long waves, currents, turbulence and vortices may be present. Therefore, the hydrodynamics to be found in the swash zone is largely determined by the boundary conditions imposed by the beach face and the inner surf zone.

In order to describe the dynamics of the swash zone, the boundary conditions at the shoreline need to be properly defined. However, a first important problem is that there is not a unique definition for the mean shoreline. Based on existing data and after a review of the instantaneous water depth and mean water surface definitions throughout the swash zone, Nielsen (1989) defines the mean shoreline as the maximum of the runup for an impermeable beach, while he considers it to be some distance seaward of the runup limit on a permeable beach and more precisely where the mean water surface intersects the beach face. Extending Nielsen's (1989) ideas, Gourlay (1992) reviews the relationship between wave set-up, runup and beach water table using

---

* Corresponding author. Tel.: +39-0521-905157; fax: +39-0521-905924.
   *E-mail addresses:* sandro.longo@unipr.it (S. Longo), petti@uniud.it (M. Petti), losadai@unican.es (I.J. Losada).
   [1] Tel.: +39-0432-558-712; fax: +39-0432-558-700.
   [2] Fax: +34-942-201860.

laboratory observations in beaches formed from various beach materials under similar wave conditions.

Brocchini and Peregrine (1996) give several possible definitions of mean shoreline based on either kinematic flow properties such as time or phase average of the waterline position or on dynamic flow properties of the swash zone, involving mass or momentum fluxes. The different possible definitions are analysed and discussed. In order to provide a simplified model of the swash zone, helpful for many wave-resolving numerical models, Brocchini and Peregrine (1996) suggest averaging the basic flow equations across the swash zone. It is found that for modelling purposes the lower boundary of the swash zone is the most convenient to take as a boundary.

Furthermore, after further averaging over short waves to obtain boundary conditions for wave-averaged models, it is shown that in addition to the kinematic type of boundary condition for a simple rigid boundary, two further conditions are found necessary to determine the changing position of the swash zone boundary and the longshore flow in the swash zone. These are boundary conditions for the long-wave motion and for the lower limit of the swash zone if the short waves have a 'known' description. These boundary conditions are obtained writing the mass balance, the onshore momentum balance and the longshore momentum balance referring to the lower limit of the swash zone.

The importance of the swash zone is widely recognised especially in the presence of a movable bottom, as with natural beaches, because a consistent part of the sediment transport takes place in it. It is well known that the intense fluid/sediment interaction that takes place in the nearshore region results in sediment suspension and transport that modifies the shoreline morphology. In this regard, the swash zone plays a very important role because it is the region of shoreline erosion and accretion. Furthermore, swash processes determine whether sediment is stored on the upper beach or is instead returned to the inner surf zone and potentially transported offshore acting as a sediment conduit between the upper beach and the surf zone (Puleo et al., 2000).

According to Thornton and Abdelrahman (1991), sediment transport in the swash zone may be considered a stirring of the sediments by energetic swash and a net transport due to mean longshore currents.

As wave breaking takes place, bore formation starts. The turbulence associated to the shoreward moving bores may reach the bed being an important mechanism to generate sediment suspension in the swash zone. Based on this process, Puleo et al. (2000) introduce a possible definition of the seaward boundary for the swash zone as "the region where the bore turbulence begins to affect local processes of sediment transport significantly". Based on field data from swash sediment transport study, Puleo et al. (2000) showed that uprush and backwash dynamics differ, observing differences in the amount of sediment suspended and the shape of the suspension profiles. Specifically, they have shown that the uprush transport is significantly influenced by bore turbulence, which travels over a very shallow bed during uprush occurrence spreading high turbulence levels towards the bed. This process could result in entraining or maintaining high quantities of suspended sediment. Therefore, bore turbulence is a dominant process in the uprush sediment transport, playing a more important role than boundary layer shear stress.

The shoreline motion is also a diagnostic of the offshore wave motion, in the sense that it is strictly related to the forcing waves. Offshore wave characteristics can be recovered from swash zone motion only if a non-linear inverse problem is solved. This is hardly doable in the case of complex topography and strong wave–wave interaction. The engineering cases that require beach runup estimates include the design of artificial beaches, the modelling of beach and dune erosion and the estimation of overtopping and breaching of dunes. See Douglass (1990) for a review focused on the practical importance of runup estimates.

The importance of the swash zone as a boundary region is also being recognised. The swash zone represents a boundary of the integration domain of the mathematical models, in which proper boundary conditions have to be imposed.

Most of the studies of the swash zone focus mainly on the water line evolution, starting with the classical analytical solution of Carrier and Greenspan (1958) for non-breaking periodic standing waves of finite amplitude on a uniform slope beach. A weakly 3-D extension (longshore components of velocity, etc., small with respect to the crosshore correspondent terms) of Carrier and Greenspan analytical solution is illustrated

by Brocchini and Peregrine (1996). Other available numerical solutions include the effects of wave breaking, bottom friction, turbulence and vorticity. In the past few decades, several field and laboratory experiments were carried out in order to detect the hydrodynamic processes taking place in the swash area. The experiments were usually carried out in laboratories, due to the difficulties in monitoring natural sites especially in the case of detailed fluid flow measurements, but several field campaigns were also conducted (George et al., 1994; Rodriguez et al., 1999).

Although the shoreline motion can be driven by non-breaking waves, most situations of practical interest are when the runup/rundown movement is strongly modulated and modified by waves breaking in shallow water. For this reason, the dynamics of wave breaking in shallow water is of specific interest (see Fig. 1). During breaking, the organised and mainly irrotational motion of the waves is transformed into vorticity, turbulence, and currents and is thereby re-organised into different patterns. Turbulence in the inner surf zone may be advected in the swash zone, and bore collapse, bed friction and the backwash bores are other sources of turbulence (e.g. Puleo et al., 2000). The theoretical approach to turbulence after breaking has often raised matters of further investigation, concerning, for example, the generation of wall jets, hydraulic jumps, bores and wakes, whose dynamics are similar in several aspects to the fluid dynamics in the swash

area. In addition, during breaking, a huge amount of air is entrained in the water body, and depending on the kind of breaking, participates in the global surf zone dynamics. Air bubbles are usually considered tracers of the vortices that can be easily observed with the naked eye, although there have been some attempts to include the air contribution in the overall dynamics by defining a two-phase model. In such cases, the representation of sediment transport in such a system should be treated as a three-phase system.

In the present review, attention is focused on turbulence in the surf and swash zone, highlighting the different phenomena that generate turbulence and the interaction of the free surface with the bottom. Section 2 introduces the analogies of flow field typical of the surf zone with other better-known flow fields and summarises the field and laboratory experiments. Section 3 is devoted to the analysis of flow field, turbulence and vorticity, with two subsections for turbulence and mean motion separation and turbulence scales.

Section 4 describes the techniques for measuring the most important state variables in the surf and in the swash area.

Section 5 is devoted to air entrapment at the free surface. The conclusions are presented in Section 6.

Reference is made to some review papers on related topics, including Peregrine (1983), Battjes (1988), Hamm et al. (1993), Banner and Peregrine (1993) and Thorpe (1995). Most of the papers in the Reference



Fig. 1. Small waves breaking on a gentle sandy beach.

Section are cited and discussed in the manuscript. A few of them are included as additional references.

## 2. Analogies of the flow field in the surf zone with other flow fields and experiments

Several models of wave breaking represent some well-known turbulence structures such as mixing layers, hydraulic jumps and submerged jets. All these turbulence structures are characterised by similarity assumptions for the mean flow and for turbulent shear stress. See Tennekes and Lumley (1972), Rajaratnam (1976), and Madsen (1981) for a widespread review of similarity methods in turbulence phenomena. Peregrine and Svendsen (1978) proposed that flow in a breaking wave is in part like a mixing layer and in part like a wake, and many experiments support this idea, at least qualitatively. Hoyt and Sellin (1989) carried out visual observations of turbulence in a hydraulic jump in a small flume. Comparing their observations with photos of gas mixing layers, the authors suggested that the hydraulics jump is a rather extreme example of a mixing layer flow with the heavier, faster fluid (water) below and the lighter, slower fluid (air) above, with an estimated ratio between air velocity to water velocity before the jump equal to 1%. Yeh and Mok (1990) and several other authors proposed similarity between a bore and a hydraulic jump. Nevertheless, there are several differences between the two flow fields due to the different boundary conditions. After imposing a Galilean transformation to follow the bore motion, the bottom appears to move with the same celerity as the bore, whereas the bottom is stationary in the case of a hydraulic jump. The main differences, as pointed out by Yeh and Mok (1990), refer to findings that indicated the following.

• The velocity profile in a hydraulic jump resembles that of a wall jet, whereas in a bore it resembles that of a wake. Velocity has a maximum somewhere away from the boundary in the former (laboratory co-ordinate frame) and at the boundary in the latter (moving co-ordinate frame).

• In a hydraulic jump, the vorticity along the bottom boundary decreases in the direction of the higher depth, whereas it increases in the same direction for a bore. It also has opposite signs in the two flow fields.

• A hydraulic jump has a steady single roller, whereas a bore in a breaking wave has successive generations of rollers (and 3-D organised turbulent motion). See Nadaoka et al. (1989).

• The boundary layer can be non-existent in front of a bore moving in a fluid at rest, whereas it can be strongly developed in the lower-depth part of a hydraulic jump, and can even induce flow separation.

This last point is dramatically important in the evaluation of bottom friction.

In particular, Yeh and Mok (1990) conclude that turbulence in bores and hydraulic jumps is related to the surface roller. The surface roller takes 'generation advection' cycles. As soon as the surface roller is generated, it is convected behind the front and then is transformed into a turbulent patch with progressive deepening. Meanwhile, a new surface roller is generated. The surface roller appears non-uniform in the cross-flow direction and it must originate 3-D turbulence patches.

Experiments conducted by Resch and Leutheusser (1972) and Resch et al. (1976) for hydraulic jumps with fully turbulent inflow in a first set, and almost uniform inflow (except for a thin boundary layer) in a second set of tests, showed significant differences in the dynamics of vorticity. In the former case, vorticity was almost uniform along the vertical and limited or negligible burst phenomena occurred near the jump, whereas in the latter, vorticity was strongly convected inducing turbulence bursts. The differences in the wall boundary layer and in the vorticity structure are less evident in the case of subsequent bores approaching the beach. In this latter case, the backwash flow generates vorticity and turbulence meeting the shoreward bore. Backwash bore seems to be responsible for a double structure of the energy spectrum, representing a secondary source of energy (Petti and Longo, 2001a,b) as happens in some larger scale turbulence phenomena, e.g. river motion after a bend. Hansen and Svendsen (1984) pointed out that wall turbulence is an order of magnitude smaller than breaker-generated turbulence, making the process virtually independent of the presence of a current. Many experiments, referring only to the uprush phase, support this. During backwash, the bottom effects generally prevail, especially if free surface generated turbulence is fast decaying.

In a recent paper, Svendsen et al. (2000) analysed in detail velocity and surface measurements in three weak

turbulent hydraulic jumps using Laser Doppler Anemometry (LDA) with particular emphasis on the flow in the roller region at the turbulent front of the jump. Experimental results confirm qualitatively the hypothesis that the breaking resembles a shear-layer, showing several deviations from the flow in ordinary shear layers. In particular in a shear layer vorticity spreads symmetrically downward and upward by diffusive mechanism, whereas in a hydraulic jump the strong turbulence in the roller enhances vorticity spreading in the entire roller region. Moreover, downstream the bottom-generated turbulence and vorticity will dominate the flow.

In addition to providing analogies with known turbulent flows, several experiments were dedicated to measuring the detailed structure of the turbulent flow field in a breaker. Mostly, measurements with LDA or hot films were performed with 2-D arrays, with few attempts to measure 3-D velocity components. 3-D measurements are rare and in most cases, the global turbulent kinetic energy is extrapolated having measured only the kinetic energy of the two main components of the flow. A table with the relative strength of the three fluctuating components for a wide class of free turbulence and wall turbulence is reported in Svendsen (1987). It indicates that the real turbulent kinetic energy is from 30% to 50% higher than that computed using the two main components of fluctuating velocity (33% in the case of isotropic turbulence). In a rare case, Nakagawa (1983) carried out flow metering in 3-D measuring the flow drag on three tension threads. Recent experiments with macroturbulence measurements, conducted by Rodriguez et al. (1999), show that in the middle surf zone the turbulence anisotropy possesses the structure of a plane-wake almost uniformly along the vertical. Using the data from Aono and Hattori (1984) and Nadaoka (1986) for spilling breakers, they also propose a spatial distribution of the ratio between horizontal and vertical fluctuating velocity as shown below:

$$u'/w' = 1.35 + 0.02z/h - 0.24(x_b - x)/L \qquad (1)$$

with $z$ vertical elevation from the seabed, $h$ the water depth, $(x_b - x)$ is the distance from the mean breaking point position and $L$ is the wavelength. Far away from the breaker, the relation suggests an inversion of the relationship between the fluctuating components, especially near the surface.

Several researchers used a submerged hydrofoil to generate spilling-type breakers (Duncan, 1981; Battjes and Sakai, 1981). Duncan (1981) used a towed hydrofoil and found that the breaking produced a shearing force along the forward face of the wave. A turbulent wake was left behind, with a momentum deficit roughly equal to the maximum momentum flux of a Stokes wave with the same speed as the breaker. The vertical thickness of the wake increased according to the square root of the distance behind the wave. Battjes and Sakai (1981) found that the region downstream of the breaker has a high degree of self-similarity in the mean velocity, turbulence intensity and shear layer, similar to a wake.

Specific interest should be devoted to bottom friction. Bottom friction is strongly related to wall boundary layer processes. In accelerated flow, forces due to acceleration work conservatively, whereas forces due to resistance are dissipative. Following a classical paper by Rouse (1965) for a swash zone flow field, the resistance law can be expressed as:

$$\frac{\partial F/\partial s}{\rho U^2 h} = \phi\left(\frac{K}{h}, \xi, \frac{\rho U h}{\mu}, \frac{U}{\sqrt{gh}}, \frac{\partial h/\partial t}{U}\right) \qquad (2)$$

where $\partial F/\partial s$ is the force per unit length, which when multiplied by the mean flow velocity yields the rate of energy dissipation:

$$\frac{U\partial F/\partial s}{\rho g Q} = -\frac{\partial H}{\partial s} \qquad (3)$$

where $Q$ is the flow discharge, $K$ is the bottom roughness, $\xi$ is a non-dimensional parameter related to the bottom profile, $h$ is the water depth, $U$ is a velocity scale, $\mu$ is the fluid viscosity and $g$ is gravity, $-\partial H/\partial s$ is the part of longitudinal slope of the line of total head corresponding to the local dissipation rate in unsteady flow. The dependence on the relative roughness $K/h$ and Reynolds number $\rho U h/\mu$ is well studied. The dependence on the Froude number seems to be important only for very high values that eventually can lead to free surface instabilities as roll waves. Froude number in the swash zone in the lab can exceed the value of 2, which is the critical Froude number for roll waves development in wide channels and which is also a suggested limiting value for bores on natural

beach (Svendsen et al., 1978; Yeh and Mok, 1990). Nevertheless, there are contradictory findings about the effect of the Froude number on friction factor (Brock, 1966). Moreover, the length required for roll waves to develop is of several thousands the normal depth, whereas the swash zone extension is usually few hundreds the normal water depth. The last non-dimensional term is related to acceleration or deceleration, which in turn induces a pressure gradient on the boundary layer. It is well known that self-similar solutions for boundary layer in the presence of a pressure gradient can be obtained only for specific conditions. As a consequence, the general form of Eq. (2) is not known. The complexity is further increased by flow reversal inducing a zero friction factor and boundary layer explosion, as well as by external turbulence acting on the boundary layer.

Tardu and Binder (1993) studied the wall shear stress modulation in unsteady turbulent flow due to high external imposed frequencies. They found that the reaction of the turbulence in unsteady wall flows depends strongly on the imposed frequency. The effect of the externally generated turbulence on a wall boundary layer was analysed by Kozakiewicz et al. (1998) who carried out experiments generating turbulence with a grid fixed on the upper lid of an oscillating tunnel, measuring the velocity with an LDA system. The global effect is expressed in terms of increased effective bottom roughness. Externally generated turbulence also induces an earlier transition to turbulence of the boundary layer.

Grain size, permeability and saturation degree are expected to influence the boundary layer, percolation, water table dynamics and turbulence generation. For a review of the boundary layer processes, see Elfrink and Baldock (2001) in this volume.

Several authors (especially to analyse its effect on wave runup and water table dynamics) have addressed the influence of beach permeability. Beach water table dynamics have been studied experimentally in the field and modelled by several authors (Turner, 1995; Turner and Nielsen, 1997; Turner and Masselink, 1998).

According to Packwood (1983), in general, infiltration/exfiltration leads to minimal changes in the overall swash hydrodynamics. However, it may become important for shingle beaches where the flow across the beach surface may be relevant.

Furthermore, for highly permeable layers of relevant width as in shingle beaches or coastal structures, the wave breaking process in swash zone may be completely changed.

Recently, Losada et al. (2000) presented a study of undertow, mean water level fluctuations and turbulence carried out in a wave flume for waves breaking on a 1:20 sloped bottom covered with thin porous layers of different characteristics. The free surface was measured using capacitance wave gauges at different locations and several velocity profiles were obtained using a 2-D Laser Doppler Velocimeter (LDV). The study indicates the differences in the dynamics of the mean flows and turbulence between the impermeable and porous bottoms.

The analysis of the turbulent kinetic energy shows that for a plunging breaker, the turbulence intensity has a maximum value located at the wave crest position for the two different porous layers considered. The turbulent kinetic energy in the cross-shore direction is multiplied by 1.33 according to Stive and Wind (1982) in order to take into account possible alongshore contributions.

Furthermore, the turbulent kinetic energy rate decreases with increasing pore size being transported in the off-shore direction for spilling breakers and in-shore in plunging breakers as shown by Ting and Kirby (1994) for impermeable bottoms.

Turbulence production sources are the free surface due to the breaking process and the bottom due to the presence of the porous layer. It has to be pointed out that due to the oscillatory character of the flow, the porous layer contributes twice as a source of turbulence generation over a wave period. These two different mechanisms interact heavily when the water depth is small or the breaking is violent.

In addition, a strong interaction with sediments is expected. Turbulence influences sediment transport and is itself modulated by grains in the flow field. The level of fluid–particles interaction depends on the sediment volume concentration, which in the swash zone can reach high values typical of slurries.

## 3. Flow field structure, vorticity and turbulence

An important forcing of the shoreline motion is wave breaking. Some waves break in shallow water,

some of them break at the water's edge and in other circumstances waves do not break at all. The last case occurs with steep beach slopes, incident waves with low steepness (or long waves) and very dissipative beds in front of a beach that are able to dissipate most of the incoming wave energy. In most cases, wave breaking develops in the surf zone and propagates into the inner surf zone like a bore, reaching the beach face in the swash zone. For wave breaking at or near the shoreline, the inner surf zone is absent. The analysis of the generation and evolution of breakers and bores is thus essential to understand the flow field characteristics in the swash zone.

The literature on wave breaking is quite extensive and detailed, see Peregrine (1983) for a description of breaking waves on beaches. Banner and Phillips (1974) state that breaking in deep water is more sporadic than breaking in shallow water. The latter is triggered by the bottom and is more predictable, although the simple question 'where breaking starts' is far from having a unique answer, even in controlled physical experiments. The breaker types are classified as spilling, where the water spills down the front face, plunging, with a jet emanating from the front crest and collapsing. The collapsing breaker occurs at the water's edge. Tallent et al. (1989) documented with high-speed video the geometry of breaking solitary waves and breaking periodic waves in very shallow water, also including some measurements on the splash up. The average eddy length scale ranges between 0.8 and 0.5 times the breaker height. Wang et al. (1994), using a numerical tank, analysed the effects of wave grouping on breaking and the dynamics of breaking waves. Kolaini and Tulin (1995) experimentally verified that a small jet formed at the wave crest at the inception of breaking. This jet led to the formation of a turbulent spilling breaker. They also verified the strong sensitivity of breaking characteristics to the disturbances left in the water by preceding breakers.

Non-breaking waves can be described using potential theory in most of the flow field except near the bottom and near the free surface, where vorticity develops and is confined to a boundary layer. As long as the details near the free surface (e.g. necessary for wind–wave interaction) and/or near the bottom (e.g. necessary for sediment transport analysis) are not of interest, the potential theory approach is sufficient.

After breaking, 'waves' and 'eddies', essentially a potential component and a rotational component of the flow field, are intimately mixed. There have been several attempts to separate the two components in laboratory data, starting from Dean's (1965) stream-function method applicable in the case of non-breaking progressive waves with permanent shape. Thornton (1979) proposed a method to evaluate the potential component as the part coherent with the free surface elevation, but it is clearly based on the assumption that the rotational component does not affect the free surface. Nadaoka (1986) developed a method to calculate the irrotational component with a Fourier decomposition of the flow field; the spectrum of the potential field is calculated using velocity data measured at a level where vorticity is practically zero. The overall procedure requires a permanent shape wave, which is not the case with a breaker. However, the effect of this limitation seems to have a limited influence, according to several tests performed by Iwagaki and Sakai (1974).

Vorticity near a fixed boundary is widely studied and is not considered further in this paper. Less studied is vorticity near the free surface and its mechanism of generation is still a matter of debate. In the case of overturning breaking waves, vorticity is topologically induced by the presence of an air cylinder (e.g. Hornung et al., 1995). Yeh (1991) argued that a baroclinic torque is the mechanism of vorticity generation at the free surface due to the presence of a non-parallel pressure gradient and density gradient in front of the bore. According to Longuet-Higgins (1992), vorticity is generated at the free surface with intensity proportional to the tangential velocity and local curvature. Steepening of the wave naturally induces high curvature and consequently strong vorticity. This is also confirmed by the experiments of Lin and Rockwell (1995) (hereafter LR). Dabiri and Gharib (1997) (hereafter DG) carried out experiments using Particle Image Velocimetry (PIV) on spilling wave breaking generated by an acceleration of the fluid stream forced through a honeycomb section; the pressure drop and the consequent increase in velocity induces a spilling breaking. They mainly found that the generation of vorticity, as well as the initiation of breaking, do not coincide with the stagnation point, and that this is due to the deceleration and not to the sharp curvature on the free surface. The apparent

contrast with experiments by LR is explained considering that in DG experiments deceleration along the free surface occurs over a distance one order of magnitude higher than in LR. Due to measurement resolution limitations, LR could not distinguish the stagnation point and the deceleration peak, and essentially their breaker can be considered a limiting case of DG breaker. The flux of vorticity into the flow is primarily due to viscous effects. A surface fluid layer is accelerated by viscous forces in order to bring the tangential stress close to the tangential stress at the surface (usually zero). Then the free surface fluid decelerates with respect to the fluid beneath it, creating a sharp velocity gradient growing into a shear layer and convecting the vorticity downstream. In the case of capillary waves, the vorticity is due to the free surface curvature and is confined to a region within the capillary amplitude, without injection into the flow.

It appears that the role of the free surface is not merely that of a boundary, as clearly indicated in numerous works on the physics of free-surface turbulence (FST), progressed in recent years by the development of remote sensing techniques. An entire Euromech Colloquium (2000) was devoted to the interaction of strong turbulence with free surfaces. Essentially, the available models of the free surface identify a boundary layer where vorticity is anisotropic, caused by the dynamic zero-stress boundary conditions, inside a thicker layer due to the kinematic boundary condition at the free surface. In this thicker layer, an increase of the horizontal velocity fluctuations at the expense of the vertical fluctuations takes place. Some hairpin-shaped vortex structures develop inside the surface layer and evolve losing their heads, connecting to the free surface and orienting the two legs almost perpendicularly to the free surface. For those vortices, the dissipation rate is extremely low after connection to the free surface, inducing a strong persistence (Shen et al., 1999). The existence of these vertical vortices, having random number and location, was documented by Chang and Liu (1998), through PIV measurements under breaking waves. The analysis of vorticity effect on mass transport shows that vorticity induces an onshoreward flux beneath the crest, in addition to the flux due to the potential flow field, the so-called Stokes drift. In addition, the momentum transport is increased in the area where

vorticity is high and the wave profile is smoother than the corresponding profile consistent with the irrotational field component. The maximum water level is smaller than the corresponding one in an irrotational field, confirming a higher efficiency in transforming potential energy into kinetic energy (Nadaoka, 1986).

Vorticity evolution is essentially 3-D, because the main mechanism of energy transfer from the mean motion to vortices is the vortex stretching, which is a 3-D phenomenon. Miller (1968) documented the presence of multiple vortices in bores. The structure of the vortices in breaking waves was analysed by Nadaoka (1986) and Nadaoka et al. (1989). They discovered the existence of 'plural horizontal vortices' (as a contradiction to Svendsen's 'singular surface roller'), parallel to the wave front, and oblique descending eddies, aligned to the principal axis of velocity deformation (Fig. 2). The first family is clearly related to the geometry of the breaking and was already suggested by Sawaragi and Iwata (1974) for plunging breakers in the outer region. The second family can be interpreted by adopting the energy cascade model, with macrovortices having axes parallel to the axis of deformation being the most effective in extracting energy from the mean flow.
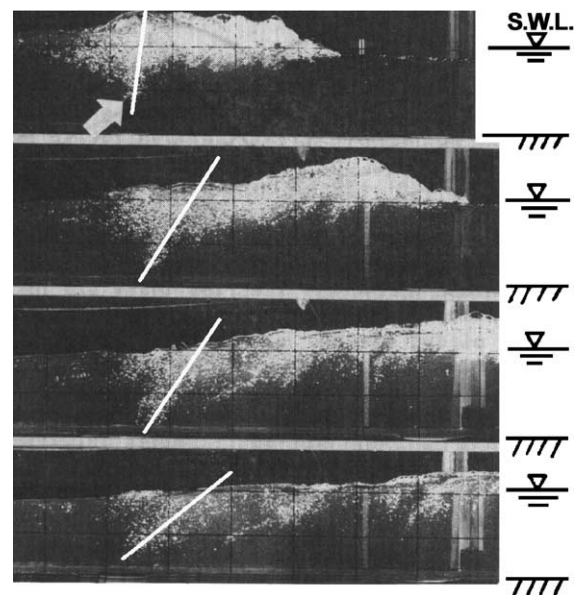


Fig. 2. Oblique descending eddies in breaking waves. The white lines represent the axis of one of the vortices (partially modified from Nadaoka, 1986, with permission).

See Peregrine (1999) for a description of vorticity generation by bores and by finite breaking wave crests.

## 3.1. Turbulence and mean motion separation

The separation of turbulence from the mean flow and other organised motions of unsteady flows is still debated and several methods have been used and widely discussed.

The classical averaging operator for periodic flows is the phase average but application to periodic waves can give large errors in the evaluation of the wave profile (Petti and Longo, 2001b). More appropriate techniques might be:

1)  the Variable Interval Time Averaging in which the phase average is modified by introducing as a trigger a reference event important for the phenomenon under investigation;
2)  the Moving Average which concentrates on local time regions.

Several operators in the frequency domain have also been used. A direct operation of filtering was suggested by Nadaoka and Kondoh (1982). As the authors explain, the method misses low frequency turbulence associated with large-scale eddies present under a bore. A more sophisticated approach is that due to Thornton (1979), and to Hattori and Aono (1985).

The technique is based on the assumption that turbulence does not influence the free surface. This is the main limitation, considering that often the free surface is strongly distorted by micro and macro turbulence.

The approach of George et al. (1994) is based on an analysis of the energy dissipation. Microvortices of high-frequency turbulence dissipate most energy, whereas at the scales of both the wave and the macrovortices energy is simply extracted from the mean motion. The overall process is conceptually correct but, unfortunately, is based on some assumptions seldom verified, especially in the laboratory, due to the existence of an inertial subrange in the spectrum, that only occurs in flows with high Reynolds number (at least $10^5$).

A mixed approach is due to Rodriguez et al. (1999), who computed the theoretical velocity spectrum by transforming the measured water elevation spectrum through a linear model. The theoretical velocity spectrum is then compared to the measured velocity spectrum with differences attributed to the turbulence. The model is globally tied in linear approximation (hardly sustainable in breaking and post-breaking conditions) and zero coherence between water surface elevation and turbulence, i.e. such that turbulence does not affect the free surface.

## 3.2. Turbulence scales

Assessment of turbulence takes advantage of dimensional analysis to define the scales of the phenomenon. A common picture of turbulence in a flow field includes the presence of macrovortices having integral length scale $\Lambda$ and velocity scale $u$, extracting energy from the mean flow and transferring it to smaller vortices to reach the dissipation scale. At the dissipation scale, viscosity acts in transferring kinetic energy into pure thermodynamic energy. The expected turbulent velocity scale after breaking can be obtained equating the integral dissipation in a bore to the energy contained in the macrovortices (see Fredsøe and Deigaard, 1992). Under several assumptions, the resulting turbulence velocity scale is expressed as (pp. 113):

$$u \propto H\left(\frac{g}{hT}\right)^{1/3} \tag{4}$$

where $H$ is the wave height, $T$ is the wave period and $h$ is the local water depth.

George et al. (1994) under the hypothesis that wave energy dissipation is completely due to turbulence with a depth-averaged dissipation rate based on the energy balance in a hydraulic jump, evaluated the turbulence velocity scale (depth mean value) as:

$$u = \frac{H_s}{h} B \sqrt{\frac{3}{8}\alpha} \left(\frac{w_b}{2T} gh^2\right)^{1/3} \tag{5}$$

where $H_s$ is the significant wave height, $B$ is a breaker coefficient related to the intensity of wave breaking (0.4–0.9), $\alpha$ is the one dimensional Kolmogorov constant (nominally 0.5), and $w_b$ is the fraction of broken waves, ranging from 0.1 to 1.0. They also proposed to compute the turbulence intensity considering only the dissipative range of the wave-number spectrum. The results obtained using both approaches are nearly equivalent.

Ting and Kirby (1995, 1996) carried out several experiments and mainly clarified the difference of the turbulence regime between spilling and plunging breakers, the former showing a larger time variation of turbulence than the latter, which dies out between two breakers. Turbulent kinetic energy is diffused seaward for the spilling and convected landward by the organised wave-induced flow for the plunging. In the latter case, it is strongly dependent on its history. They found a velocity scale of turbulence on the order of $1/10–1/5$ of the wave celerity. Assuming the integral length scale to be a fraction of the local water level (from 0.5 to 1), a crude estimate of the time scale of the macrovortices is $t \cong 0.25–10h/c$. This is consistent with many laboratory measurements.

Sakai et al. (1982) proposed a phase-resolving model of turbulence using a wake adjusted turbulence model. Deigaard et al. (1986) used a simplified form of the 1-D kinetic energy transport equation introducing a production term proportional to the dissipated energy in the breaker that is quadratic in time and space, acting for a limited part of the wave period. The results of all these models, including a model by Svendsen (1987), are compared in Tada et al. (1990).

The spatial variation of turbulence onshore and offshore was investigated extensively by Hattori and Aono (1985) who found turbulence intensities increasing in the outer region and stable in the inner region. This is more evident below the still water level than near the bottom. The patterns are quite similar for the horizontal and vertical velocity fluctuations. Also, Ting and Kirby (1994, 1995) found that under spilling breakers turbulence and undertow variations in the vertical are much higher than under plunging breakers, whereby the plunging rapidly saturates the vertical, in an interval time equal to:

$$\frac{t_d}{T} \cong 2\frac{d/L}{H/d} \tag{6}$$

in which $t_d$ is the time of diffusion, $d$ is the mean local water depth (equal to the still water depth plus set-up or set-down).

Some information on the dependence of the mean turbulent kinetic energy on bed slope is reported by Svendsen (1987). Using simplifying assumptions, he found that the mean turbulent kinetic energy is proportional to the bed slope raised to a power $n$ ranging

from 2/3 to 1. The physical explanation is that the steeper the slope, the shorter the distance of spreading of the energy flux and higher is the mean value of turbulent energy.

The natural integral length scale is the water depth. According to Cox et al. (1994), the length scale increases from the outer to the inner surf zone (in the lab), being in the range $0.04–0.18h$. Higher values can be reached in the field, up to $0.43h$ in the swash zone (Flick and George, 1990); further field experiments revealed a length scale of $0.58h$ in the inner surf zone (Rodriguez et al., 1999). Smith et al. (1993) assume a length scale equal to $H_{rms}$. Pedersen et al. (1998), using two Laser Doppler Anemometers (LDAs), measured the spatial correlation between the vertical velocity components in two sections of the inner surf zone under spilling breakers and found a value about $0.3h$, similar to the values obtained for open channel flows except near the bottom. Petti and Longo (2001b) carried out experiments in the lab under plunging–collapsing breakers. They adopted a time correlation and Taylor's hypothesis of frozen turbulence and found streamwise horizontal length macro scales in the swash zone near the bottom around $\sim 1.5\delta$ (where $\delta$ is the maximum local water level, assumed as a significant scale), rapidly decreasing upward. Rodriguez et al. (1999), aiming to fit several experimental data, proposed the following expression:

$$\Lambda/h = a_1 + a_2 H_{rms}/h + a_3 U_{orb}/c \tag{7}$$

in which $U_{orb}$ is the r.m.s. orbital velocity under wave crest. The coefficients obtained through a multiple regression analysis have values equal to $a_1 = 0.28$, $a_2 = -0.84$ and $a_3 = 2.82$.

## 4. Measurements techniques in the surf and swash area

The difficulty of making measurements directly inside a highly dynamic zone such as the swash zone is well known. Therefore, most of the existing experience is based on measurements of the shoreline oscillations.

The time series of surface elevation is usually obtained through twin wire gauges, of capacitance or resistance type. For resistance/capacitance type, the

space between the wave gauges cannot be less than a minimum value in order to avoid interference. In addition, digital (short-contact) wave staffs used and subsurface pressure gauges have been used. Measurements with pressure gauges are based on the assumption of hydrostatic pressure distribution and can be questionable especially in the breaking area, where curvature of water surface is significant and a lot of air bubbles are present. Shoreline position was measured through a digital comb-type, shorting contact wave staff (Van Dorn, 1976). The comb tips had a spatial resolution of 2 or 4 cm, and cleared the surface by about 1 mm. Both the spatial resolution and the spurious contact especially in the retreating film during backwash can underestimate the shoreline level. The sensor can be embedded in the beach, with sensor tip projected less than 1 mm above the beach surface (Yeh et al., 1989). In the presence of alternatively dry and wet bed, the boundary effects can induce a strong non-linear response. A special device was used in a study by Synolakis (1987), which consisted of an array of capacitance gauges made of steel wire fitted in a glass capillary tube. The gauges were supported by a π-shape aluminium frame and were used with the tip 1 mm above the tank bottom surface. They could all be calibrated at the same time with sophisticated electronics to avoid cross-talk. Comparison of the results with video-image analysis gave errors within 3%.

For field measurements, Holland et al. (1995) used several arrays of twin wires stacked at elevations of 5, 10, 15, 20 and 25 cm above the bed, with rods supporting 60 m long wires. The sensors were described in Guza and Thornton (1982) including a survey of the problems encountered using similar arrays for several months. Runup can also be measured using video cameras overlooking the area or time-lapse photography. See Holman and Guza (1984) for a comparison of the two techniques.

Velocity and turbulence measurements in bores or in breakers are usually carried out using the techniques used in other flow fields. Laser Doppler Velocimetry is widely used, with several limitations in the aerated region due to bubble presence (Nadaoka and Kondoh, 1982; Cox et al., 1994; Losada et al., 2000).

Hot wire and hot film anemometry is also used, especially in laboratories given the well-known problems in calibration of such instruments, but also in the field (George et al. 1994). Nakagawa (1983) used a tension thread flowmeter for measuring the three components of velocity under breaking waves.

Acoustic Doppler Velocimeters (ADV), able to measure 3-D velocity in a single point with a frequency response up to 30 Hz, and electromagnetic sensors, with a good frequency response up to 20 Hz are also available. See Rodriguez et al. (1999) for a comparison of the two instruments' performances. Acoustic Doppler Profilers (ADP) are also becoming available, which are able to measure velocity in several points along the ultrasound beam with a frequency response up to several tens of Hz. In Fig. 3, the horizontal velocity $U$ and the vertical velocity $V$ measured using ADP in a breaking wave (a) and in the subsequent bore (b) is shown (Longo et al., 2000).

Amongst optical methods, the most widely used in laboratory experiments is Particle Image Velocimetry. See Lin and Rockwell (1994) for high-image-density PIV of a breaking wave, Chang and Liu (1998), Emarat and Greated (1999), Emarat et al. (1999), and Greated and Emarat (2000) for application of PIV in measuring breaking wave characteristics.

The main problem in using all these devices is the presence of air bubbles. The air bubbles have different effects on the output signal, depending on the electronics of the instrument, and generally, they induce noise spikes and signal clipping if bubble presence saturates the system, or results in temporary signal dropouts. Signal dropouts can also be easily generated due to mass absence. Seldom the signal velocity with bubble presence is a measure of the bubble velocity. The techniques for data correction and validation are standard, but they cannot overcome the lack of data in strongly aerated regions.

Measurements of air bubble concentrations have been carried out using conductive probes, as in Lamarre (1993). The bubble size population was measured by Kolaini (1998) through a high-speed video camera with fibre optic cables.

For a thorough review on hydrodynamic and sediment transport measurements in the swash zone, see Butt and Russel (2000).

## 5. The effect of air entrapment

During breaking, a huge quantity of air is often entrained (Fig. 4), especially in the field where the
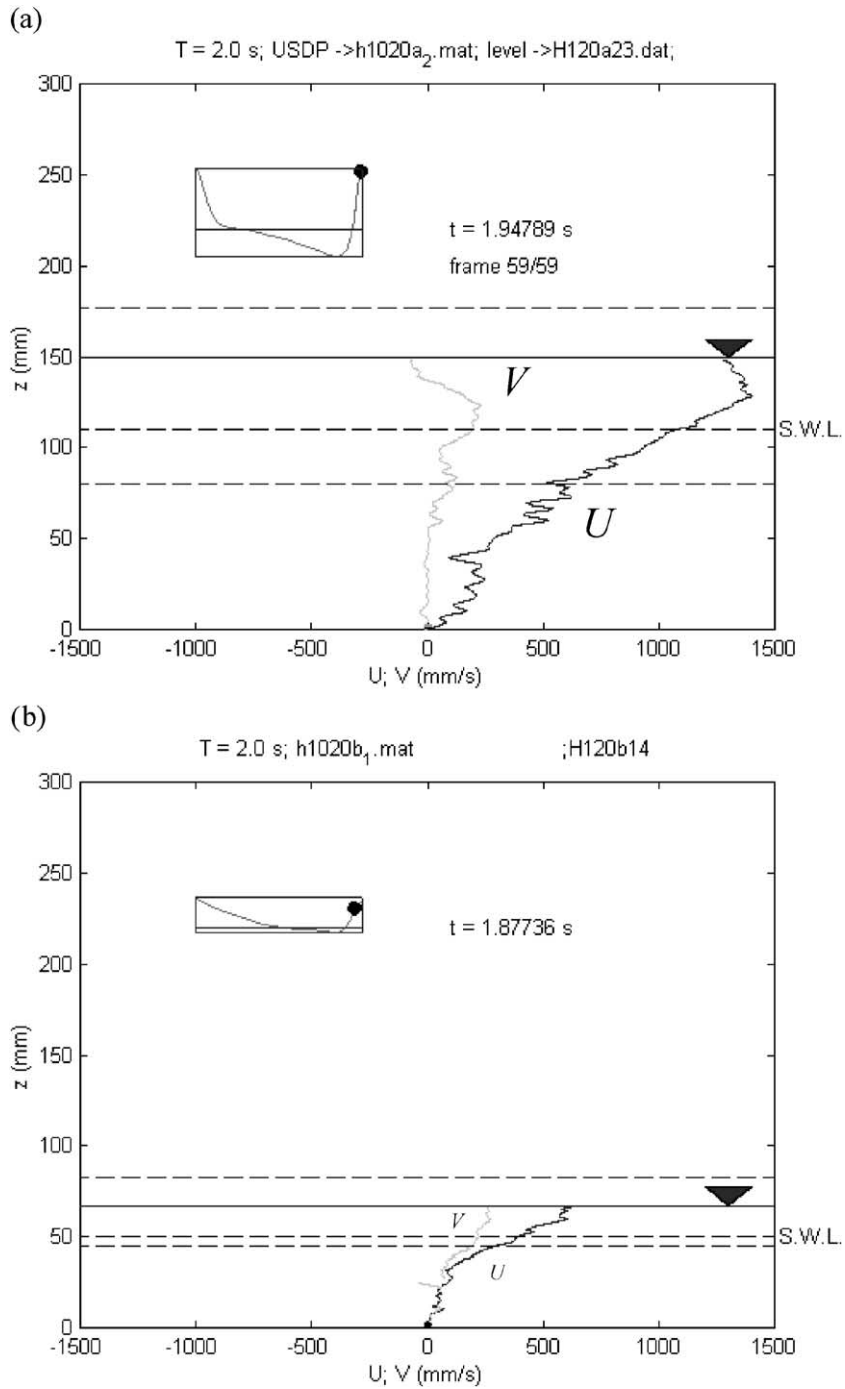
Fig. 3. Horizontal and vertical velocity profiles in a breaker (a) and in the subsequent bore (b) obtained through UltraSound Doppler Profiler. $T = 2.0$ s, $H = 10$ cm, bottom slope 1:20. The average free surface profile and the phase are shown in the subplots (Longo et al., 2000).

Fig. 4. Air–water front of the water tongue during swash. Laboratory experiments.

surface tension effects have minor relevance. In the swash tongue evolution, the air bubbles accumulate at the waterfront. This is due to the buoyancy effect, with bubbles moving toward the free surface where the fluid velocity is higher, and where they still survive because of surface tension effects. The rate of collapse of the bubbles is comparable to the rate of convection of new bubbles, and the front appears continuously foamed. In backwash, there is an inversion of the rate of convection, and the bubbles disappear in a short time, except for the smaller bubbles that can persist for longer periods. Some large bubbles also remain attached to sand, if present, on the bottom.

The presence of air bubbles itself is not an indicator of turbulence because strong turbulence can be present even without bubbles (Peregrine and Svendsen, 1978; a set-up without bubbles is proposed to simplify measurements). Nevertheless, breakers are easily recognised due to the formation of whitecaps, whose coverage and lifetime seem to have a correlation with salinity (Monahan and Zeitlow, 1969). The present knowledge of air entrapment in free surface flows is much more developed for high-velocity flows of fresh water in open channels, such as spillways and chutes. The common assumption is that air is entrained when the kinetic energy of the surface eddies exceeds the surface tension and the turbulent boundary layer reaches the free surface (Afshar et al., 1994). Local aeration by impinging jets is also very common, with vortices in the intensive shear layer at the penetration point strong enough to entrain air at their core. Volkart (1980) experimentally analysed the mechanism of air bubble entrapment in self-aerated flows in a steep partially filled pipe, using a stroboscopic technique. He found that the air bubble consequent to drops impinging on the water surface is always bigger than the pertinent water drop and also computed the minimum vertical distance of a water drop in order to form an air bubble. The size of the air bubble increases with the vertical distance of the water drop. The minimum vertical distance decreases for larger drops.

Cummings and Chanson (1999) investigated the inception of air bubble entrapment by a supported planar plunging water jet, almost perpendicular to the free surface of water at rest in a pool. The inception velocity strongly increases for decreasing turbulence level in the jet. In addition, the mechanism of air entrapment appeared influenced by foam presence at the intersection of the jet with the water in the pool. In addition, Zhu et al. (2000) presented an experimental and theoretical study on air entrapment by liquid jets at a free surface (perpendicular). They also found that a water jet without disturbances has a limited efficiency in air entrapment. The volume of entrapped air is approximately proportional to the size of the disturbances.

The other extreme situation, with jet flow issued parallel to the free surface, was experimentally analysed by Walker et al. (1995). They analysed qualitative features of the subsurface flow and free surface disturbances and measured all six Reynolds stresses using a 3-D Laser Doppler. Depending on Froude and Reynolds numbers, they mainly found that energy is preferentially transferred to turbulence or to free-surface disturbances (waves).

An air bubble plume is always present in plunging waves: the air cylinder is entrained, then becomes unstable due to centrifugal and gravitation effects and collapses with a finger-like bubble structure. A detailed experiment on this topic is reported in Lamarre (1993) and Kolaini (1998). Lamarre (1993) found that immediately beneath breaking waves a high air volumetric concentration can be recorded within the first metre of the surface, equivalent to up to 24% in the ocean (which is several orders of magnitude higher than the time-averaged values reported by other authors, e.g. Walsh and Mulhearn, 1987). In 2-D laboratory experiments in fresh water, the entrained air is proportional to the energy dissipated, with the formation of a primary and a secondary bubble plume.

The primary bubble plume moves with a celerity around 0.7 times the wave celerity, deepens at a speed of $\sim 0.2H/T$ with a maximum penetration depth between $0.2H$ and $0.35H$ (the wave length can also be used as an important scaling factor) and loses 95% of the entrained air during one wave period; the minimum void concentration is always higher than 1%. Similar results were obtained in 3-D laboratory experiments, with faster expansion of the bubble plume with respect to the 2-D case but the secondary bubble plume was almost negligible. Several researchers found that fresh and seawater bubble families have different distributions and that bubble densities can differ by an order of magnitude, although the behaviour immediately after breaking seems to be comparable. The recorded bubble population is various, with bubbles of a few micrometres to few a millimetres, and is expected to have strong variations during a wave period due to big bubbles collapsing or small bubble coalescence and different rising velocities. The bubble size spectrum shifts to smaller bubbles in salt water. The difference seems to be related to the absence of bubble coalescence in salt water, due to organic active materials which are able to reduce the surface tension and to prevent thin films from rupturing (Kitchener, 1964) or to electric repulsion between bubbles due to the preferential ions deposition over the surface (Pounder, 1986). In addition, Su et al. (1994) recorded high void fractions, up to 60% at a depth of 25 cm and wind speed of 15 m/s. A significant fraction, from 30% to 50%, of the energy dissipated during breaking is work against buoyancy. Part of the energy is radiated in pressure waves because of single bubble oscillations or collective plume oscillations, part is transferred back to the fluid during bubble rising. This phenomenon can be used to explain the need to reduce the production term in several turbulence models in order to fit the experimental data (see Tada et al., 1990). See Thorpe (1995) and Melville (1996) for reviews on dynamic processes of transfer at the sea surface and the role of surface-wave breaking in air–sea interaction.

## 6. Conclusions

In the last few decades, lab and field experimental works on the breaking process and swash dynamics have significantly increased our knowledge on these topics.

The basic approach of describing a highly complex dynamic system by analysing individually the different processes interrelated under controlled conditions has given promising descriptive and quantitative results regarding many characteristics of the flow field.

Turbulence measurements and analysis in the swash zone in the lab are increasing in number. With respect to surf zone, the bottom turbulence plays an important role, depending on the kind of breaking, and is dominant during downrush. The limited water depth enhances the interaction between free surface, bottom and turbulence, with a general stirring of the length scales. The strong non-stationarity of the flow field and the generally limited Reynolds number prevent an equilibrium range in turbulence spectra.

Although potential sources of turbulence in the swash zone are more or less well known, a detailed description of the turbulence processes—their interrelation with larger scale processes, the role of suspended sediment, the effect of bottom permeability, air entrapment and the corresponding modelling—is still at an early stage.

Field measurements have been relatively few in numbers and there is a clear need to improve the currently available instrumentation in order to achieve high quality measurements in the swash zone. Furthermore, in order to develop validated swash zone models, the collection of comprehensive data sets is necessary. Therefore, the physical processes have to be clearly identified in order to select the proper magnitudes to be measured and data analysis techniques.

Too little work has examined the effects of air entrainment at the free surface on turbulence dynamics. The gross effect of air bubbles is to dissipate and accumulate energy as work against buoyancy, up to 50% according to some field studies (Lamarre, 1993). During bubble rising, a small amount of energy is transferred back to the fluid, as well as radiating pressure waves. The effects of air can only be studied using large/full scale models possibly with salt water (if breaking in sea waves is the main topic). In addition, more sophisticated instruments and techniques need to be developed in order to measure the state variables in a two-phase or three-phase system if sediment grains are present.

In addition, the importance of extremely dense water/sand mixtures in the swash zone has to be recognised and addressed especially in experimental research. Sediment transport in sheet-flow condition at the bottom and very high volume concentration of suspended sediments dramatically modifies the structure of turbulence, with grains actively involved in the transport processes. A huge amount of flux momentum is due to grains suspended in the flow field and to grain–grain collision, making the mixture behave as a non-Newtonian dilatant fluid. The unsteadiness of the flow is a major complexity and should be taken into account in modelling the dynamics of sediment transport. The impossibility of scaling several rheological effects, including friction amongst grains, also suggests the need for field experiments at a prototype scale.

## 7. Uncited references

Baldock et al., 1997
Battjes, 1975
Carlson, 1984
Chanson, 1997
Cox et al., 1992
Flick et al., 1981
Foote and Horn, 1999
Guza and Thornton, 1980
Guza and Thornton, 1981
Guza et al., 1984
Hasselmann, 1971
Hibberd and Peregrine, 1979
Janssen, 1986
Kobayashi, 1999
Kobayashi and Wurjanto, 1992
Kobayashi et al., 1989
Launder and Spalding, 1972
Longuet-Higgins, 1973
Longuet-Higgins, 1996
Longuet-Higgins and Turner, 1974
Madsen and Svendsen, 1983
Matsunaga and Honji, 1980
Mizuguchi, 1984
Mizuguchi, 1986
Narayan, 1975
Okayasu et al., 1986
Olmez and Milgram, 1992
Packwood and Peregrine, 1980
Rajaratnam, 1965
Rao et al., 1970
Raubenheimer and Guza, 1996
Raubenheimer and Guza, 1995
Roos and Battjes, 1976
Sakai et al., 1986
Sarpkaya, 1996
Sonu et al., 1974
Stive, 1984
Svendsen and Madsen, 1984
Svendsen and Putrevu, 1995
Svendsen et al., 1996
Thornton and Guza, 1982
Tsai and Yue, 1996
Whitam, 1974
Wu, 1995

## List of symbols

| | |
|---|---|
| ADV | Acoustic Doppler Velocimeter |
| ADP | Acoustic Doppler Profiler |
| $a_1$, $a_2$, $a_3$, $\alpha$, $B$ | Coefficients |
| $\delta$ | Maximum local water depth (m) |
| $\varepsilon$ | Turbulent energy dissipation rate ($m^2/s^3$) |
| $\xi$ | Parameter in the resistance law |
| $\eta$ | Water level (m) |
| $\kappa$ | Turbulent kinetic energy ($m^2/s^2$) |
| $\Lambda$ | macro scale length (m) |
| $c$ | Wave phase celerity (m/s) |
| $d$ | Mean local water depth (m) |
| $F$ | Force (N) |
| $f$ | Frequency (Hz) |
| FST | Free surface turbulence |
| $g$ | Gravitational acceleration ($m/s^2$) |
| $h$ | Water depth (m) |
| $H$ | Total head (m) |
| $H$, $H_s$, $H_{rms}$ | Wave height, significant wave height, r.m.s. wave height (m) |
| $k$, $k_0$ | Wave number, cut-off wave number ($m^{-1}$) |
| $K$ | Bottom roughness (m) |
| $L$ | Wave length (m) |
| LDV, LDA | Laser Doppler Velocimetry, Anemometry |
| PIV | Particle Image Velocimetry |
| $Q$ | Flow discharge ($m^3/s$) |
| $s$ | Curvilinear abscissa (m) |
| $T$ | Wave period (s) |
| $t$, $t_d$ | Time variable, time of diffusion (s) |
| $U$, $V$ | Horizontal velocity, vertical velocity (m/s) |

$u$, $u_\varepsilon$     Turbulent velocity scale, turbulent velocity scale based on dissipation (m/s)

$u'$, $v'$, $w'$ Fluctuating velocity (m/s)

$w_b$        Fraction of broken waves

$x$, $y$, $z$, $x_i$ Spatial co-ordinates (m)

## Acknowledgements

## References

Afshar, N.R., Asawa, G.L., Ranga Raju, K.G., 1994. Air concentration distribution in self-aerated flow. J. Hydraul. Res. 32, 623–631.

Aono, T., Hattori, M., 1984. Experimental study on the spatial characteristics of turbulence due to breaking waves. 30th J. Conf. Coastal Eng., JSCE, 25–29 (in Japanese).

Baldock, T.E., Holmes, P., Horn, D.P., 1997. Low frequency swash motion induced by wave grouping. Coastal Eng. 32, 197–222.

Banner, M.L., Peregrine, D.H., 1993. Wave breaking in deep water. Annu. Rev. Fluid Mech. 25, 373–397.

Banner, M.L., Phillips, O.M., 1974. On the incipient breaking of small scale waves. J. Fluid Mech. 65, 647–656.

Battjes, J.A., 1975. Modelling of turbulence in the surf-zone. Proc. of Symposium on Modelling Techniques, ASCE, San Francisco, 1050–1061.

Battjes, J.A., 1988. Surf-zone dynamics. Annu. Rev. Fluid Mech. 20, 257–293.

Battjes, J.A., Sakai, T., 1981. Velocity field in a steady breaker. J. Fluid Mech. 111, 121–137.

Brocchini, M., Peregrine, D.H., 1996. Integral flow properties of the swash zone and averaging. J. Fluid Mech. 317, 241–273.

Brock, R.R., 1966. Discussion of critical analysis of open channel resistance by Hunter Rouse. Proc. ASCE, J. of the Hydraulic Division, 92, HY2, 403–409.

Butt, T., Russell, P., 2000. Hydrodynamics and cross-shore sediment transport in the swash-zone of natural beaches: a review. J. Coastal Res. 16 (2), 255–268.

Carlson, C.T., 1984. Field studies of run-up on dissipative beaches. Proc. 19th Intl. Conf. on Coast. Eng., ASCE, 399–414.

Carrier, C.F., Greenspan, H.P., 1958. Water waves of finite amplitude on a sloping beach. J. Fluid Mech. 4, 97–109.

Chang, K.-A., Liu, P.L.-F., 1998. Velocity, acceleration and vorticity under a breaking wave. Phys. Fluids 10, 327–329.

Chanson, H., 1997. Air Bubble Entrainment in Free Surface Turbulent Shear Flow. Academic Press, London, UK, p. 401 ISBN 0-12-168110-6.

Cox, D.T., Kobayashi, N., Wurjanto, A., 1992. Irregular wave transformation processes in surf and swash zones. Proc. 23rd Intl. Conf. on Coast. Eng., ASCE, 156–169.

Cox, D.T., Kobayashi, N., Okayasu, A., 1994. Vertical variations of fluid velocities and shear stress in surf zones. Proc. 24th Intl. Conf. on Coast. Eng., ASCE, 98–112.

Cummings, P.D., Chanson, H., 1999. An experimental study of individual air bubble entrainment at a planar plunging jet. Chem. Eng. Res. Design, Part A 77 (A2), 159–164.

Dabiri, D., Gharib, M., 1997. Experimental investigation of the vorticity generation within a spilling water wave. J. Fluid Mech. 330, 113–139.

Dean, R.G., 1965. Stream function representation of nonlinear ocean waves. J. Geophys. Res. 70 (18), 4561–4572.

Deigaard, R., Fredsøe, J., Hedegaard, I.B., 1986. Suspended sediment in the surf zone. J. Waterw., Port, Coast. Ocean Eng. 112 (1), 115–128.

Douglass, S.L., 1990. Estimating run-up on beaches: a review of the state of the art. U.S. Army, Waterways Experiment Station Report CERC-90-3, Vicksburg.

Duncan, J.H., 1981. An experimental investigation of wave breaking produced by a towed hydrofoil. Proc. R. Soc. London, Ser. A 377, 331–348.

Elfrink, B., Baldock, T., 2001. Hydrodynamics and sediment transport in the swash zone: a review and perspectives. Coastal Eng., SASME Special Issue, this issue.

Emarat, N., Greated, C.A., 1999. Turbulence study in breaking waves on a beach using PIVProc. of 3rd Int. Workshop on Particle Image Velocimetry, Santa Barbara, California, 16–18 September.

Emarat, N., Christensen, E.D., Forehand, D.I.M., 1999. A Study of Plunging Breaker Mechanics by PIV Measurements and a Navier–Stokes Solver. Abstract for the 27th Intl. Conf. on Coast. Eng., ASCE, Sydney, Australia.

Euromech Colloquium 416, 2000. Interaction of strong turbulence with free surface. Genova, Sep. 17th–20th. Book of abstracts.

Flick, R.E., George, R.A., 1990. Turbulence scales in the surf and swash. Proc. 22nd Intl. Conf. on Coast. Eng., ASCE, 557–569.

Flick, R.E., Guza, R.T., Inman, D.L., 1981. Elevation and velocity measurements in laboratory shoaling waves. J. Geophys. Res. 86 (C5), 4149–4160.

Foote, M., Horn, D., 1999. Video measurements of swash zone hydrodynamics. Geomorphology 29, 59–76.

Fredsøe, J., Deigaard, R., 1992. Mechanics of Coastal Sediment Transport. Advanced Series on Ocean Engineering, vol. 3. World Scientific, ISBN 981-02-0840-5, 369 pp.

George, R., Flick, R.E., Guza, R.T., 1994. Observation of turbulence in the surf zone. J. Geophys. Res. 99 (C1), 801–810.

Gourlay, M.R., 1992. Wave set-up, wave run-up and beach water table: interaction between surf zone hydraulics and groundwater hydraulics. Coastal Eng. 17, 93–144.

Greated, C.A., Emarat, N., 2000. Optical studies of wave kinematics. In: Liu, P.L.-F. (Ed.), Advances in Coastal and Ocean

Engineering. World Scientific, vol. 6, 223 pp. + xi, ISBN981-02-4236-4.

Guza, R.T., Thornton, E.B., 1980. Local and shoaled comparisons of sea surface elevations, pressures and velocities. J. Geophys., 86.

Guza, R.T., Thornton, E.B., 1981. Wave set-up on a natural beach. J. Geophys. Res. 86 (C5), 4133–4137.

Guza, R.T., Thornton, E.B., 1982. Swash oscillations on a natural beach. J. Geophys. Res. 87, 483–491.

Guza, R.T., Thornton, E.B., Holman, R.A., 1984. Swash on steep and shallow beaches. Proc. 19th Intl. Conf. on Coast. Eng., ASCE, 708–723.

Hamm, L., Madsen, P.A., Peregrine, D.H., 1993. Wave transformation in the nearshore: a review. Coastal Eng. 21, 5–39.

Hansen, J.B., Svendsen, I.A., 1984. A theorethical and experimental study of the undertow. Proc. 19th Intl. Conf. on Coast. Eng., ASCE, 2246–2262.

Hasselmann, K., 1971. On the mass and momentum transfer between short gravity waves and larger-scale motions. J. Fluid Mech. 50, 189–205.

Hattori, M., Aono, T., 1985. Experimental study on turbulence structures under spilling breakers. In: Toba, F., Mitsuyasu, H. (Eds.), The Ocean Surface. Reidel, Dordrecht, pp. 419–424.

Hibberd, S., Peregrine, D.H., 1979. Surf and runup on a beach: a uniform bore. J. Fluid Mech. 95, 323–345.

Holland, K.T., Raubenheimer, B., Guza, R.T., Holman, R.A., 1995. Run-up kinematics on a natural beach. J. Geophys. Res. 100 (C3), 4985–4993.

Holman, R.A., Guza, R.T., 1984. Measuring run-up on a natural beach. Coastal Eng. 8, 129–140.

Hornung, H.G., Willert, C., Turner, S., 1995. The flow field downstream of a hydraulic jump. J. Fluid Mech. 287, 299–316.

Hoyt, J.W., Sellin, R.H.J., 1989. Hydraulic jumps as "Mixing Layer". J. Hydraul. Eng., ASCE 115 (12), 1607–1614.

Iwagaki, Y., Sakai, T., 1974. Representation of water particle velocity of breaking waves on beaches by Dean's stream function method. Proc. 21st Jap. Conf. on Coastal Eng. JSCE, 27–32.

Janssen, P.C.M., 1986. Laboratory observations of the kinematics in the aereated region of breaking waves. Coastal Eng. 9 (5), 453–477.

Kitchener, J.A., 1964. Foams and free liquid film. Recent Progress in Surface Science, vol. 1. Academic Press, New York, pp. 51–93.

Kobayashi, N., 1999. Wave runup and overtopping on beaches and coastal structuresAdvances in Coastal and Ocean Engineering, vol. 5. World Scientific, Singapore, pp. 95–154.

Kobayashi, N., Wurjanto, A., 1992. Irregular wave setup and runup on beaches. J. Waterw., Port, Coast. Ocean Eng. 118, 368–386.

Kobayashi, N., DeSilva, G.S., Watson, K.D., 1989. Wave transformation and swash oscillation on gentle and steep slopes. J. Geophys. Res. 94 (C1), 951–966.

Kolaini, A.R., 1998. Sound radiation by various types of laboratory breaking waves in fresh and salt water. J. Acoust. Soc. Am. 103 (1), 300–308.

Kolaini, A.R., Tulin, M.P., 1995. Laboratory measurements of breaking inception and post-breaking dynamics of steep short-crested waves. Int. J. Offshore Polar Eng. 5 (3), 212–218.

Kozakiewicz, A., Sumer, B.M., Fredsøe, J., Deigaard, R., 1998. Effect of external generated turbulence on wave boundary layer. Report No. 77, Inst. of Hydrodynamics and Hydraulic Engineering, ISVA, Techn. Univ. Denmark.

Lamarre, E., 1993. An experimental study of air entrainment by breaking waves. PhD Thesis, MIT, 327 pp.

Launder, B.E., Spalding, D.B., 1972. Mathematical Models of Turbulence Academic Press, New York.

Lin, J.-C., Rockwell, D., 1994. Instantaneous structure of a breaking wave. Phys. Fluids 6 (9), 2877–2879.

Lin, J.-C., Rockwell, D., 1995. Evolution of a quasi-steady breaking wave. J. Fluid Mech. 302, 29–44.

Longo, S., Losada, I.J., Petti, M., Pasotti, N., Lara, J.L., 2000. Measurements of breaking waves and bores through a USD velocity profiler. Technical Report UPR/UCa_01_2001, University of Parma, University of Cantabria.

Longuet-Higgins, M.S., 1973. A model of flow separation at a free surface. J. Fluid Mech. 57, 129–148.

Longuet-Higgins, M.S., 1992. Capillary rollers and bores. J. Fluid Mech. 240, 659–679.

Longuet-Higgins, M.S., 1996. Surface manifestations on turbulent flows. J. Fluid Mech. 308, 15–29.

Longuet-Higgins, M.S., Turner, J.S., 1974. An 'entraining plume' model of a spilling breaker. J. Fluid Mech. 63, 1–20.

Losada, I.J., Lara, J.L., Losada, M.A., 2000. Experimental study on the influence of bottom permeability on wave breaking and associated processes. Proc. 27th Intl. Conf. on Coast. Eng., ASCE, 706–719.

Madsen, P.A., 1981. A model for a turbulent bore. Series paper 28, Inst. Hydrodyn. and Hydraul. Engng., Tech. Univ. Denmark.

Madsen, P.A., Svendsen, I.A., 1983. Turbulent bores and hydraulic jumps. J. Fluid Mech. 129, 1–25.

Matsunaga, N., Honji, H., 1980. The backwash vortex. J. Fluid Mech. 99, 813–815.

Melville, W.K., 1996. The role of surface wave breaking in air–sea interaction. Annu. Rev. Fluid Mech. 28, 279–323.

Miller, R.L., 1968. Experimental determination of run-up of undular and fully developed bore. J. Geophys. Res. 73, 4497–4510.

Mizuguchi, M., 1984. Swash on a natural beach. Proc. 19th Intl. Conf. on Coast. Eng., ASCE, 679–694.

Mizuguchi, M., 1986. Experimental study on kinematics and dynamics of wave breaking. Proc. 20th Intl. Conf. on Coast. Eng., ASCE, 589–603.

Monahan, E.C., Zeitlow, C.R., 1969. Laboratory comparisons of fresh water and sal water whitecap. J. Geophys. Res. 74, 6961–6966.

Nadaoka, K., 1986. A fundamental study on shoaling and velocity field structure of water waves in the nearshore zone. Tech. Report No. 36, Dept. Civ. Engrg., Tokyo Inst. Tech., 125 pp.

Nadaoka, K., Kondoh, T., 1982. Laboratory measurements of velocity field structure in the surf zone by LDV. Coastal Eng. Jpn. 25, 125–145.

Nadaoka, K., Hino, M., Koyano, Y., 1989. Structure of the turbulent flow field under breaking waves in the surf zone. J. Fluid Mech. 204, 359–387.

Nakagawa, T., 1983. On characteristics of the water-particle velocity in a plunging breaker. J. Fluid Mech. 126, 251–268.

Narayan, R., 1975. Wall jet analogy to hydraulic jump. J. Hydraul. Div., Am. Soc. Civ. Eng. 101 (HY3), 347–359.

Nielsen, P., 1989. Wave setup and runup: an integrated approach. Coastal Engineering, vol. 13. Elsevier, Amsterdam, pp. 1–9.

Okayasu, A., Shibayama, T., Numiura, N., 1986. Velocity field under plunging waves. Proc. 20th Intl. Conf. on Coast. Eng., ASCE, 660–674.

Olmez, H.S., Milgram, J.H., 1992. An experimental study of attenuation of short water waves by turbulence. J. Fluid Mech. 239, 133–156.

Packwood, A., 1983. The influence of beach porosity on wave uprush and backwash. Coastal Eng. 7, 29–40.

Packwood, A., Peregrine, D.H., 1980. The propagation of solitary waves and bores over a porous bed. Coastal Eng. 3, 221–242.

Pedersen, C., Deigaard, R., Sutherland, J., 1998. Measurements of the vertical correlation in turbulence under broken waves. Coastal Eng. 35, 231–249.

Peregrine, D.H., 1983. Breaking waves on beaches. Annu. Rev. Fluid Mech. 15, 149–178.

Peregrine, D.H., 1999. Large-scale vorticity generation by breakers in shallow and deep water. Eur. J. Mech. B: Fluids 18, 403–408.

Peregrine, D.H., Svendsen, I.A., 1978. Spilling breakers, bores and hydraulic jumps. Proc. 16th Intl. Conf. on Coast. Eng., ASCE, 540–550.

Petti, M., Longo, S., 2001a. Hydrodynamics in the swash zone. Int. J. Offshore Polar Eng. (IJOPE) 11 (3), 27–35.

Petti, M., Longo, S., 2001b. Turbulence experiments in the swash zone. Coastal Eng. 43/1, 1–24.

Pounder, C., 1986. Sodium chloride and water temperature effects on bubbles. In: Monakan, A., Mac Niocaill, L. (Eds.), Oceanic Whitecap and Their Role in Air–Sea Exchange Processes, pp. 109–121.

Puleo, J.A., Beach, R.A., Holman, R.A., Allen, J.S., 2000. Swash zone sediment suspension and transport and the importance of bore generated turbulence. J. Geophys. Res. 105 (C7), 17021–17044.

Rajaratnam, N., 1965. The hydraulic jump as a wall jet. J. Hydraul. Div., Am. Soc. Civ. Eng. 91 (HY5), 107–131.

Rajaratnam, N., 1976. Turbulent jets. Developments in Water Science. vol. 5. Elsevier, Amsterdam.

Rao, N.S.L., Seetharamiah, K., Gangadharaiah, T., 1970. Characteristics of self-aerated flows. J. Hydraul. Div., Am. Soc. Civ. Eng. 96 (2), 331–332.

Raubenheimer, B., Guza, R.T., 1995. Swash on a gently sloping beach. J. Geophys. Res. 100, 8751–8760.

Raubenheimer, B., Guza, R.T., 1996. Observations and predictions of run-up. J. Geophys. Res. 101, 25575–25587.

Resch, F.J., Leutheusser, H.J., 1972. Reynolds stress measurements in hydraulic jumps. J. Hydraul. Res. 10, 409–430.

Resch, F.J., Leutheusser, H.J., Coantic, M., 1976. Etude de la structure cinematique et dynamique du ressant hydraulique. J. Hydraul. Res. 14, 293–319.

Rodriguez, A., Sanchez-Arcilla, A., Redondo, J.M., Mosso, C., 1999. Macroturbulence measurements with electromagnetic and ultrasonic sensors: a comparison under high-turbulent flows. Exp. Fluids 27, 31–42.

Roos, A., Battjes, J.A., 1976. Characteristics of flow in run-up of periodic waves. Proc. 15th Intl. Conf. on Coast. Eng., ASCE, 781–795.

Rouse, H., 1965. Critical analysis of open-channel resistance. J. Hydraul. Div., Am. Soc. Civ. Eng. (HY4), 4387–4412.

Sakai, T., Inada, Y., Sandanbata, I., 1982. Turbulence generated by wave breaking on beach. Proc. 18th Intl. Conf. on Coast. Eng., ASCE, 3–21.

Sakai, T., Mizutani, T., Tanaka, H., Tada, Y., 1986. Vortex formation in plunging breaker. Proc. 20th Intl. Conf. on Coast. Eng., ASCE, 711–723.

Sarpkaya, T., 1996. Vorticity, free surface and surfactants. Annu. Rev. Fluid Mech. 28, 88–128.

Sawaragi, T., Iwata, K., 1974. Turbulent effect on wave deformation after breaking. Coastal Eng. Jpn. 17, 39–49.

Shen, L., Zhang, X., Yue, D.K.P., Triantafyllou, G.S., 1999. The surface layer for free surface turbulent flows. J. Fluid Mech. 386, 167–212.

Smith, J.M., Larson, M., Kraus, N., 1993. Longshore current on a barred beach: field measurements and calculation. J. Geophys. Res. 98 (C12), 22717–22731.

Sonu, C., Pettigrew, N., Fredericks, R., 1974. Measurement of swash profile and orbital motion on the beach. Proc. Ocean Wave Measurements and Analysis Conf., ASCE, 621–638.

Stive, M.J.F., 1984. Energy dissipation in waves breaking on gentle slopes. Coastal Eng. 8, 99–127.

Stive, M.J.F., Wind, H.G., 1982. A study of radiation stress and set-up in the nearshore region. Coastal Engineering, vol. 6. Elsevier, Amsterdam, pp. 1–25.

Su, M.Y., Todoroff, D., Cartmill, J., 1994. Laboratory comparisons of acoustics and optical sensors for microbubble measurements. J. Atmos. Ocean Technol. 11 (1), 170–181.

Svendsen, I.A., 1987. Analysis of surf zone turbulence. J. Geophys. Res. 92, 5115–5124.

Svendsen, I.A., Madsen, P.A., 1984. A turbulent bore on a beach. J. Fluid Mech. 148, 73–96.

Svendsen, I.A., Putrevu, U., 1995. Surf zone hydrodynamics. Ocean Engineering Laboratory, Res. Rpt. No CACR-95-02, University of Delaware, Delaware.

Svendsen, I.A., Yu, K., Veeramony, J., 1996. A boussinesq breaking wave model with vorticity. Proc. 25th Intl. Conf. on Coast. Eng., ASCE, 1192–1204.

Svendsen, I.A., Madsen, P.A., Hansen, J., 1978. Wave characteristics in the surf zone. Proc. of the 16th Coast. Eng. Conf., ASCE, 520–539.

Svendsen, I.A., Veeramony, J., Bakunin, J., Kirby, J.T., 2000. The flow in weak turbulent hydraulic jumps. J. Fluid Mech. 418, 25–57.

Synolakis, C.E., 1987. The runup of solitary waves. J. Fluid Mech. 185, 523–545.

Tada, Y., Sakai, T., Obana, E., 1990. Variation of surf zone turbulence in a wave period. Proc. 22nd Intl. Conf. on Coast. Eng., ASCE, 716–728.

Tallent, J.R., Yamashita, T., Tsuchiya, Y., 1989. Transformation characteristics of breaking water waves. In: Torum, A., Goudmestad, O.T. (Eds.), Water Wave Kinematics. NATO ASI Series E: Applied Sciences, vol. 178, pp. 509–523.

Tardu, F.S., Binder, G., 1993. Wall shear stress modulation in un-

steady turbulent channel flow with high imposed frequencies. Phys. Fluids A 5 (8), 2028–2037.

Tennekes, H., Lumley, J.L., 1972. A First Course in Turbulence. The MIT Press, Cambridge, MA, 300 pp.

Thornton, E.B., 1979. Energetics of breaking waves in the surf zone. J. Geophys. Res. 84, 4931–4938.

Thornton, E.B., Abdelrahman, S., 1991. Sediment transport in the swash due to obliquely incident wind-waves modulated by infragravity waves. Proc. Coastal Sediments '91, 100–113.

Thornton, E.B., Guza, R.T., 1982. Energy saturation and phase speeds measured on a natural beach. J. Geophys. Res. 87 (C2), 9499–9508.

Thorpe, S.A., 1995. Dynamical processes of transfer at the sea surface. Prog. Oceanogr. 35, 315–352.

Ting, F.C.K., Kirby, J.T., 1994. Observation of undertow and turbulence in a laboratory surf zone. Coastal Eng. 24, 51–80.

Ting, F.C.K., Kirby, J.T., 1995. Dynamics of surf-zone turbulence in a strong plunging breaker. Coastal Eng. 24, 177–204.

Ting, F.C.K., Kirby, J.T., 1996. Dynamics of surf-zone turbulence in a spilling breaker. Coastal Eng. 27, 131–160.

Tsai, W.-T., Yue, D.K.P., 1996. Computations of non-linear free-surface flows. Annu. Rev. Fluid Mech. 28, 249–278.

Turner, I.L., 1995. Simulation of the influence of groundwater seepage on sediment transport by sweep of the swash across macrotidal beaches. Mar. Geol. 125, 153–174.

Turner, I.L., Masselink, G., 1998. Swash infiltration–exfiltration and sediment transport. J. Geophys. Res. 103 (C13), 30813–30824.

Turner, I.L., Nielsen, P., 1997. Rapid water table fluctuations within the beach face: implications for swash zone sediment mobility? Coastal Eng. 32, 45–59.

Van Dorn, W.G., 1976. Set-up and run-up in shoaling breakers. Proc. 15th Intl. Conf. on Coast. Eng., ASCE, 738–751.

Volkart, P., 1980. The mechanism of air bubble entrainment in self-aerated flow. Int. J. Multiphase Flow 6, 411–423.

Walker, D.T., Chen, C.-Y., Willmarth, W.W., 1995. Turbulent structure in free surface jet flows. J. Fluid Mech. 291, 223–261.

Walsh, A.L., Mulhearn, P.J., 1987. Photographic measurements of bubble populations from breaking wind waves at sea. J. Geophys. Res. 92, 14553–14565.

Wang, P., Yao, Y., Tulin, M.P., 1994. Wave group evolution, wave deformation, and breaking: simulations using LONGTANK, a numerical wave tank. Int. J. Offshore Polar Eng. 4 (3), 200–205.

Whitam, G.B., 1974. Linear and Nonlinear Waves Wiley, New York.

Wu, S., Rajaratnam, N., 1995. Free jumps, submerged jumps and wall jets. J. Hydraul. Res. 33 (2), 197–212.

Yeh, H., 1991. Vorticity generation in bores. Proc. R. Soc. London, Ser. A 432, 215–231.

Yeh, H.H., Mok, K.M., 1990. On turbulence in bores. Phys. Fluids 2, 821–828.

Yeh, H.H., Ghazali, A., Marton, I., 1989. Experimental study of bore run-up. J. Fluid Mech. 206, 563–578.

Zhu, Y., Oğuz, H.N., Prosperetti, A., 2000. On the mechanism of air entrainment by liquid jets at a free surface. J. Fluid Mech. 404, 151–177.